Cancer Research

Novel *SEC61G–EGFR* Fusion Gene in Pediatric Ependymomas Discovered by Clonal Expansion of Stem Cells in Absence of Exogenous Mitogens

Tiziana Servidei[1], Daniela Meco[1], Valentina Muto[2], Alessandro Bruselles[3], Andrea Ciolfi[2], Nadia Trivieri[4], Matteo Lucchini[5], Roberta Morosetti[6], Massimiliano Mirabella[5], Maurizio Martini[7], Massimo Caldarelli[8], Anna Lasorella[9], Marco Tartaglia[2], and Riccardo Riccardi[1]

Abstract

The basis for molecular and cellular heterogeneity in ependymomas of the central nervous system is not understood. This study suggests a basis for this phenomenon in the selection for mitogen-independent (MI) stem-like cells with impaired proliferation but increased intracranial tumorigenicity. MI ependymoma cell lines created by selection for EGF/FGF2-independent proliferation exhibited constitutive activation of EGFR, AKT, and STAT3 and sensitization to the antiproliferative effects of EGFR tyrosine kinase inhibitors (TKI). One highly tumorigenic MI line harbored membrane-bound, constitutively active, truncated EGFR. Two EGFR mutants (ΔN566 and ΔN599) were identified as products of intrachromosomal rearrangements fusing the 3′ coding portion of the *EGFR* gene to the 5′-UTR of the *SEC61G*, yielding products lacking the entire extracellular ligand-binding domain of the receptor while retaining the transmembrane and tyrosine kinase domains. EGFR TKI efficiently targeted ΔN566/ΔN599-mutant–mediated signaling and prolonged the survival of mice bearing intracranial xenografts of MI cells harboring these mutations. RT-PCR sequencing of 16 childhood ependymoma samples identified *SEC61G–EGFR* chimeric mRNAs in one infratentorial ependymoma WHO III, arguing that this fusion occurs in a small proportion of these tumors. Our findings demonstrate how *in vitro* culture selections applied to genetically heterogeneous tumors can help identify focal mutations that are potentially pharmaceutically actionable in rare cancers. *Cancer Res; 77(21); 5860–72. ©2017 AACR.*

Introduction

Ependymoma is the second most common of malignant brain tumors in children, with a 5-year survival rate at approximately 50% (1–3). Mainstays of treatment are surgery and radiation, whereas chemotherapy has failed to demonstrate a clear overall survival benefit (3–6). The current histopathologic classification identifies three major ependymoma subtypes (WHO grades I, II, and III; ref. 7). However, accurate diagnosis is often challenging, because many tumors consist of intermingled areas of distinct grades (8). The integration of multidimensional genomic, epigenetic, and transcriptional data has provided evidence that ependymomas arising in the different regions of the neuroaxis are biologically and clinically distinct entities that are generated by different glial stem cell (SC) populations (8–12).

In culture, ependymoma SCs are forced into active proliferation by exogenous epidermal growth factor (EGF) through binding to its receptor EGFR (13). We have previously established 2 patient-derived ependymoma SC lines in serum-free medium with EGF/fibroblast growth factor 2 (FGF2; ref. 14). Phosphorylated EGFR was detected in both lines, which decreased after differentiation, indicating that EGFR activation is an inherent feature of stemness.

EGFR is a transmembrane tyrosine kinase composed of an extracellular ligand-binding domain at the N-terminus, a transmembrane domain, and an intracellular domain with catalytic activity (15, 16). EGF-triggered activation of EGFR initiates a cascade of downstream signals controlling cellular proliferation, differentiation, and survival. Aberrant signaling through EGFR is observed in a wide range of neoplasms and is mediated by various mechanisms, including gene amplification, receptor or ligand overexpression, and constitutive kinase activity by mutations (17). Approximately 50% of high-grade glioma shows *EGFR* amplification often associated with structural alterations. Among these, the most common is an in-frame deletion of exons 2 to 7 of the gene, resulting in the expression of the constitutively activated oncogenic EGFRvIII, which lacks 267 amino acids from the

[1]UOC Oncologia Pediatrica, Fondazione Policlinico Universitario "A. Gemelli," Rome, Italy. [2]Genetics and Rare Diseases Research Division, Ospedale Pediatrico Bambino Gesù, Rome, Italy. [3]Department of Oncology and Molecular Medicine, Istituto Superiore di Sanità, Rome, Italy. [4]Mendel Institute, IRCCS Casa Sollievo della Sofferenza, San Giovanni Rotondo, Italy. [5]Institute of Neurology, Catholic University, Rome, Italy. [6]UOC Neurologia, Fondazione Policlinico Universitario "A. Gemelli," Rome, Italy. [7]Institute of Pathology, Catholic University, Rome, Italy. [8]Institute of Neurosurgery, Catholic University, Rome, Italy. [9]Department of Pediatrics, Department of Pathology and Cell Biology, Columbia University Medical Center, New York, New York.

Note: Supplementary data for this article are available at Cancer Research Online (http://cancerres.aacrjournals.org/).

M. Tartaglia and R. Riccardi contributed equally to this article.

Corresponding Author: Tiziana Servidei, Fondazione Policlinico Universitario "A. Gemelli," Largo A. Gemelli, 8, 00168, Rome, Italy. Phone: 39-06-3015-5165; Fax: 39-06-305-2751; E-mail: tiziana.servidei@guest.policlinicogemelli.it

doi: 10.1158/0008-5472.CAN-17-0790

extracellular domain (18, 19). A role for EGFR in ependymoma pathogenesis has been inferred from its frequent overexpression in these tumors associated with worse prognosis (20, 21). However, *EGFR* gene amplification represents a rare event in ependymoma and no mutation affecting the coding sequence of the gene has been reported so far (21).

Although the dependence of brain tumor SCs on EGF for spherogenic and proliferative properties is well established, a distinguishing feature of cancerous cells is their ability to develop self-sufficiency in growth signals. Independence from exogenous mitogens has been reported in glioblastoma SCs, which retain proliferative and tumor initiation properties when grown without EGF (22, 23). Interestingly, *EGFR* amplification and EGFRvIII expression, which are usually lost in cells cultured in mitogen-enriched media, are maintained in EGF-free media (23, 24). Together, these findings indicate that culture conditions might exert either negative or positive selection pressure on genetically heterogeneous subpopulations of tumor cells.

Here, we addressed whether omission of EGF/FGF2 from SC cultures provides growth advantage to ependymoma cells that rely on autonomous proliferative/survival signaling. We established MI ependymoma lines, displaying constitutive activation of EGFR, AKT, and STAT3 and increased intracranial tumorigenicity compared with mitogen-dependent (MD) lines. In the MI line with the most malignant phenotype, we discovered an *SEC61G-EGFR* gene fusion resulting in two truncated, constitutively active receptors, EGFRΔN566 and EGFRΔN599, which lack the vast majority of the extracellular ligand-binding region. EGFRΔN566/EGFRΔN599-expressing cells were sensitive to EGFR-targeted agents both *in vitro* and *in vivo*. Notably, RT-PCR sequencing of 16 pediatric ependymomas identified *SEC61G–EGFR* chimeric mRNAs in one infratentorial WHO III tumor, indicating that this event likely occurs in a small subset of ependymomas, although its clinical relevance has yet to be defined.

Materials and Methods

Cell culture and reagents

Ependymoma SC lines EPP and EPV were established from two pediatric infratentorial ependymomas in our laboratory in 2010 and fully characterized (14). EPV-FL line was derived from one subcutaneous EPV xenograft in 2012 (Supplementary Data; Supplementary Figs. S1A and S1B). All lines were cultured in Neurocult medium (Stem Cell Technologies) supplemented with 20 ng/mL EGF (Sigma-Aldrich) and 10 ng/mL FGF2 (Promega; referred to as SC medium, SCM). MI lines were generated in 2011 to 2012 by growing the corresponding MD lines in Neurocult medium without growth factors (referred to as mitogen-free medium, MFM) for approximately 4 months. Cell lines were tested for *mycoplasma* contamination within the last 6 months with MycoSensor PCR Assay Kit (Stratagene). All experiments were performed with cells between passages 15 and 26.

The EGFR tyrosine kinase inhibitors (TKI) gefitinib and AEE788 (25) were kindly provided by AstraZeneca and Novartis Pharmaceuticals, respectively. For *in vitro* and *in viv*o studies, drugs were dissolved as previously described (14, 26).

For viability assays, cells were seeded onto 6-well plates. After 24 hours, vehicle or serial concentrations of each tested drug were added to the medium, and cells were cultured for 3 days. Cell number and viability were assessed by an automated cell counter (NucleoCounter 100TM, ChemoMetec), which allows for discrimination between live and dead cells through staining of nuclei with propidium iodide. The half-maximal inhibitory concentration (IC_{50}) was calculated using the GraphPad Prism software package version 6.0 (GraphPad Software Inc.).

Patients and tissue samples

Ependymoma surgical specimens and clinicopathologic information were collected with informed written consent in accordance with the Declaration of Helsinki. Twelve ependymomas were infratentorial, 2 were supratentorial, and 1 was spinal. Data were unavailable for 1 tumor. According to the histopathologic classification, 7 tumors were WHO grade II, while 9 tumors were anaplastic ependymoma WHO grade III.

Gene fusion analysis

Total RNA was extracted from cell lines or frozen tissues using the AllPrep DNA/RNA/Protein Kit (Qiagen). RNA sequencing was outsourced (Polo GGB). Data analysis was performed using the RNA-Seq Analysis Pipeline (27), a cloud computing web application integrating tools for quality check, identification and quantification of transcripts, and detection of alternative transcript processing. About 42M paired-end reads were obtained after quality filtering. Among them, about 94% were mapped on reference (54.9%, coding regions; 29.1%, UTR; 5.7%, introns; 8.4%, intergenic regions; 1.8%, ribosomal RNA). ChimeraScan (28) identified an *SEC61G–EGFR* fusion joining the 5′-UTR of *SEC61G* and exon 14 of *EGFR*. A total of 650 reads mapped around the identified junction, 513 of them spanning the junction itself. All the other putative fusion transcripts detected were discarded as representing technical artifacts or being associated with low-quality reads (Supplementary Table S1).

Detailed methods for the validation of the RNA-seq data and the *SEC61G–EGFR* fusion screening assay are available in Supplementary Data.

EGF stimulation and protein analysis

Ependymoma lines were cultured in MFM for 48 hours and then stimulated with 25 ng/mL EGF for different time intervals (10 minutes up to 6 hours). At the end of incubations, cells were harvested in lysis buffer or processed for multicompartmental fractionation with the Subcellular Protein Fractionation kit (Thermo Scientific). To study the effects of pharmacological inhibition, serial dilutions of EGFR TKIs were added to MFM 2 hours prior to EGF stimulation. Immunoblotting analyses were performed using standard protocols (14, 26) and the antibodies listed in Supplementary Data.

In vivo models and animal treatment

All experimental animal investigations complied with the guidelines of the Ethical Committee of Catholic University and of the "Istituto Superiore di Sanità'' (National Institute of Health, Rome, Italy; OPBA 35-01, Approval no. 243/2015). For intracranial transplantations, 3×10^5 cells/10 μL PBS were implanted into the lateral ventricle of 5-week-old male nude CD1 nu/nu mice (Charles River) as previously described (14, 26). AEE788 was administered orally (50 mg/kg daily for 5 days/week) for 4 weeks. Control group received only vehicle. Animals were monitored daily until symptomatic, when they were euthanized, and brains removed for histopathologic analysis. Survival of animals was determined using the Kaplan–Meier method.

Additional methods

Detailed methods for generation of ependymoma lines, flow cytometry, reverse transcription PCR (RT-PCR), validation of RNA-seq data, *SEC61G–EGFR* fusion screening assay, quantitative real-time PCR (qPCR), immunofluorescence analyses of human ependymomas, double-immunofluorescence analyses of cell lines and xenograft sections, subcutaneous xenografts, statistical methods, primers and antibodies used are available in Supplementary Data.

Results

MI ependymoma SCs display impaired proliferation *in vitro*, but increased intracranial tumorigenicity

To assess whether ependymoma SCs can proliferate independently of mitogen stimulation, three ependymoma lines (EPP, EPV, and EPV-FL) established in SCM were cultured in MFM for approximately 4 months. All cultures developed into permanent MI lines (EPP-MI, EPV-MI, and EPV-FL-MI), which displayed doubling times up to 3-fold longer (Fig. 1A; Supplementary Fig. S1C), and a 2- to 3-fold higher cell death rate (Fig. 1B). Acute deprivation of mitogens strongly impaired growth of MD lines, because of a time-dependent increase in cell death. Conversely, addition of mitogens slightly enhanced the proliferation rate of MI lines and significantly reduced cell death only after prolonged exposures (8–14 days). Together, these data suggest that withdrawal of exogenous mitogens exerts a positive selection pressure on MI subpopulations, in which, however, MD cells continue to form and die in the absence of growth factors, being rescued from cell death by the addition of EGF/FGF2.

Contrasting their diminished proliferative ability *in vitro*, all MI lines retained intracranial tumorigenicity. Moreover, mice engrafted with EPP-MI and EPV-FL-MI cells survived significantly shorter (median, 25 and 59 days, respectively) than mice engrafted with EPP (median 71 days, $P = 0.0007$, log-rank test) or EPV-FL cells (median 68 days, $P = 0.0105$, log-rank test; Fig. 1C). There was no significant difference between survival of mice bearing EPV or EPV-MI tumors (Supplementary Fig. S1D).

We furthered our investigation in EPP-MI and EPV-FL-MI models, which showed a more aggressive *in vivo* behavior. To

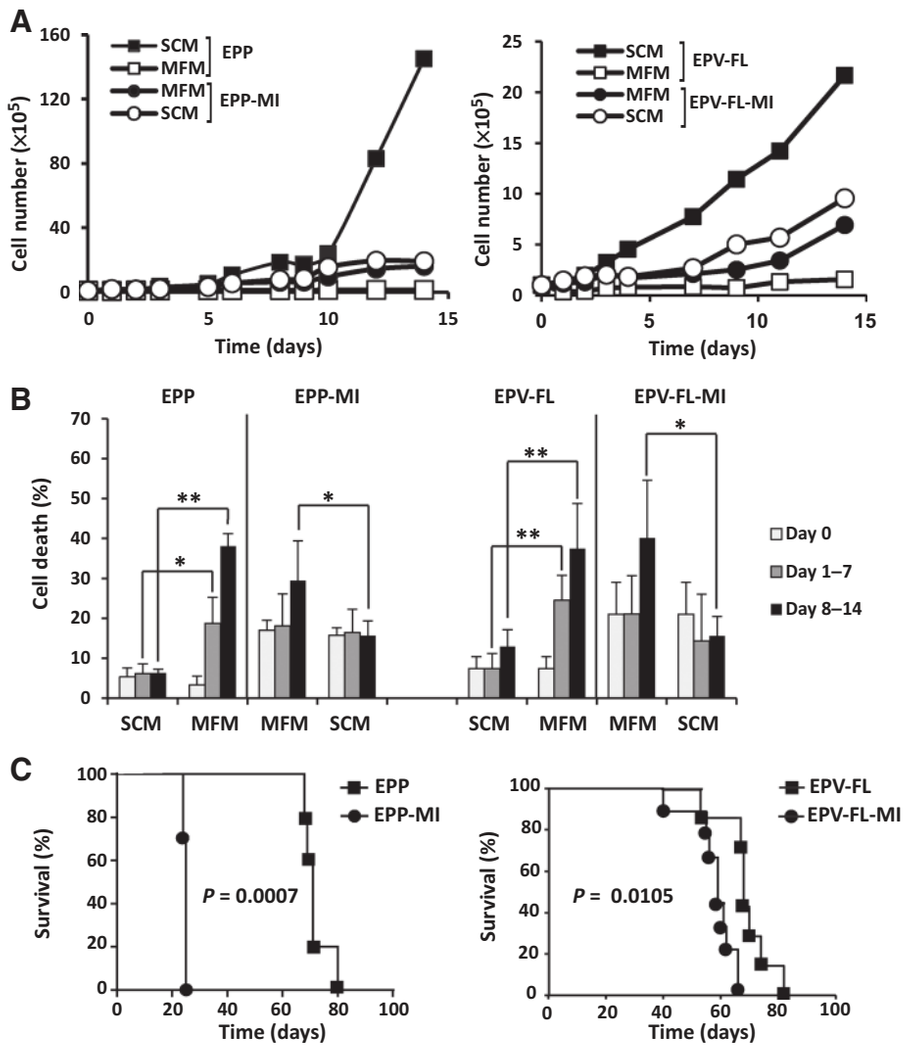

Figure 1.
MI ependymoma lines retain proliferative and tumor initiation properties. **A,** *In vitro* proliferation of paired MD and MI ependymoma lines was evaluated in their respective growth media, i.e., SCM and MFM, respectively (filled symbols). Parallel experiments were performed in the reverse conditions for each line (empty symbols). One representative experiment in triplicate is shown. **B,** Cell death of the above proliferation curves was plotted as mean ± SD through days 1 to 7 and days 8 to 14. *, $P < 0.05$; **, $P < 0.01$; Student *t* test. **C,** Survival of mice (at least, 5 mice/group) after orthotopic injection of an equal number of viable cells of the indicated lines. Mice were sacrificed when brain tumor symptoms developed. Survival was examined using the Kaplan–Meier method.

address whether enhanced tumor-initiating capability of MI lines was associated with more pronounced stemness features (9, 14), we compared mRNA expression of *CD133 (PROM1)*, *OLIG2*, *NES*, and *SOX2* in paired MD and MI lines by qPCR. The levels of these markers either decreased significantly (*CD133*, *OLIG2*, and *NES*) or were unchanged (*SOX2*) in EPP-MI cells (Fig. 2A). *CD133* and *OLIG2* transcript levels were also significantly reduced in EPV-FL-MI, with no substantial differences in *NES* and *SOX2* expression. Flow cytometric analysis confirmed that the CD133-positive fraction was reduced in MI lines (Fig. 2B). As for the markers of differentiation pathways, the oligodendroglial marker *GALC* was downregulated in both MI lines, whereas the SC/astrocytic marker *GFAP* increased in EPV-FL-MI, while decreasing in EPP-MI. The levels of the neuronal marker *TUBB3* were to the limit of detection.

The differential expression of stemness markers between MD and MI lines could be due to culture conditions. Therefore, both EPP and EPP-MI lines were grown in either SCM or MFM for 48 hours before the quantification of mRNA levels of SC markers. When lines were grown in the same culture media, a consistent and significant decrease in the expression of all the markers tested was observed in EPP-MI cells as compared with EPP (Fig. 2C).

MI ependymoma lines express constitutively active EGFR or EGFRΔN566/EGFRΔN599

Because EGF-dependent EGFR signaling is essential for the proliferation of neural and brain tumor SCs (13), we examined the expression and activation status of EGFR in MD and MI ependymoma cultures. Level of total EGFR was higher in EPV-MI and EPV-FL-MI lines as compared with parental MD lines,

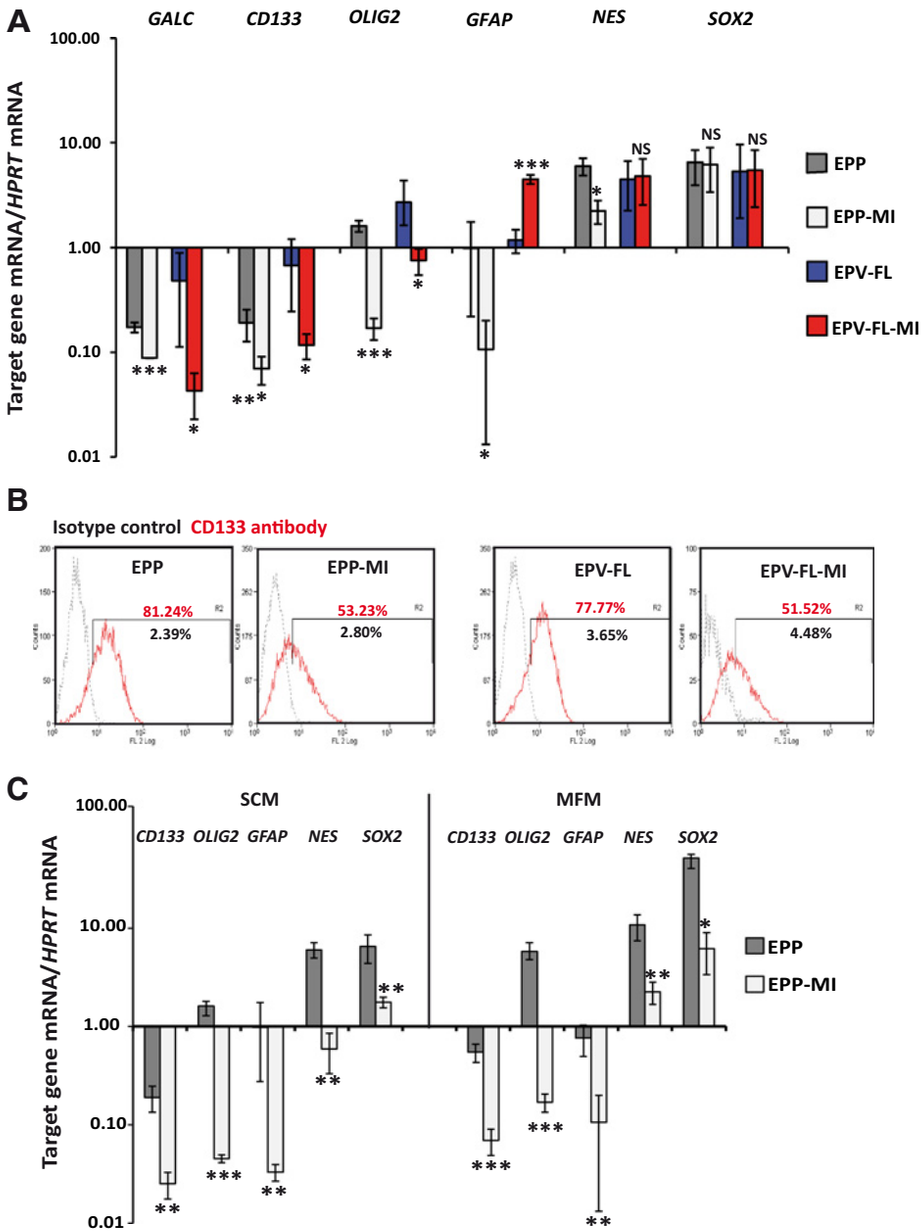

Figure 2.
Increased tumorigenicity of MI lines is not associated with a consistent modulation of stemness/differentiation markers. **A,** mRNA quantification of the indicated neural SC markers (*CD133, OLIG2, NES,* and *SOX2*) and differentiation markers (*GALC* and *GFAP*) in paired MD and MI ependymoma lines cultured in their respective proliferation media, i.e., SCM and MFM, respectively. **B,** Flow cytometric analysis of CD133 expression in ependymoma lines. Cells were stained with fluorescence-conjugated antibodies and detected by flow cytometry. **C,** qPCR analysis of the expression of the indicated genes in EPP and EPP-MI lines, both grown in either SCM or MFM for 48 hours. In **A** and **C**, results are represented as mRNA levels relative to *HPRT* expression (mean ± SD; at least, $n = 6$). Student *t* test was used for statistical significance: NS, not significant; *, $P < 0.05$; **, $P < 0.001$; ***, $P < 0.0001$; significantly different from gene expression levels in the corresponding MD line.

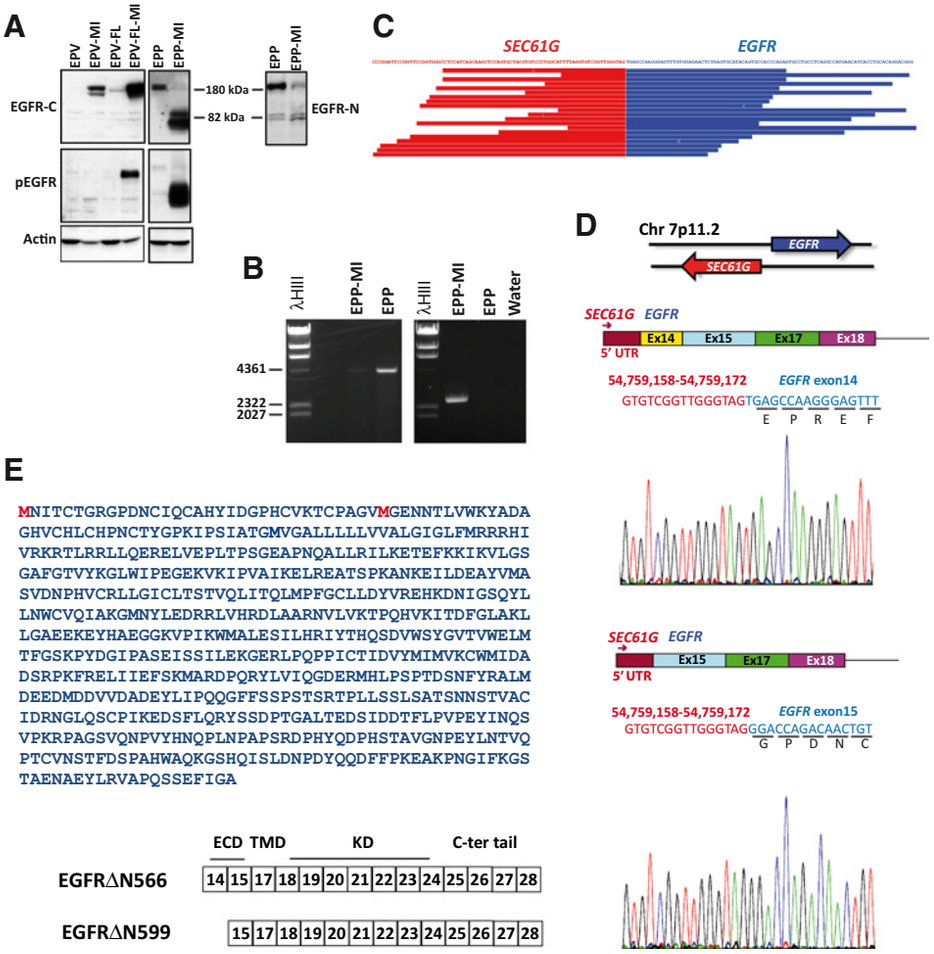

Figure 3.
Constitutively active EGFR or EGFRΔN566/EGFRΔN599 are present in MI ependymoma lines. **A,** Detection of total and phosphorylated EGFR (pEGFR) in MD and MI ependymoma lines. Antibodies raised against the C-terminus (EGFR-C) or N-terminus (EGFR-N) were used for total EGFR. Actin was used as a loading control. **B,** PCR amplicons of full-length *EGFR* (left) and *SEC61G–EGFR* (right) from cDNAs from the indicated ependymoma lines. Water was used as a negative control for the PCR. **C,** Split reads are shown aligning on the breakpoint. **D,** Electropherograms at the breakpoint of two distinct *SEC61G–EGFR* fusion products detected in EPP-MI cells. **E,** EGFRΔN566/EGFRΔN599 sequences and schematics, showing the extracellular domain (ECD), the transmembrane (TMD), and kinase (KD) domains of the gene fusion products. In red, the first methionine of EGFRΔN566 and EGFRΔN599, respectively.

whereas it was much lower in EPP-MI (Fig. 3A). Detection of EGFR in EPV cells, which express low levels of the receptor (14), required prolonged film exposure times. Activated EGFR was observed only in EPV-FL-MI, in spite of the absence of exogenous EGF. Of interest, in EPP-MI cells, a highly expressed protein of approximately 80 kDa was recognized by antibodies to either EGFR-C terminal or phosphorylated EGFR (pEGFR), but was not by an antibody recognizing the N-terminal of the receptor (Fig. 3A). Differential EGFR expression among lines was confirmed at mRNA levels by qPCR with two interexonic Taqman assays, corresponding to the coding regions of *EGFR* N-terminal (exons 4–5) or C-terminal (exons 27–28; Supplementary Fig. S2A). Both amplicons were upregulated in EPV-MI and EPV-FL-MI as compared with MD lines, with the highest levels in EPV-FL-MI. In EPP-MI cells, only the expression of the C-terminal coding region increased, whereas the amplicon encompassing exons 4 to 5 was highly diminished. Together, these data suggested that EPP-MI cells harbored truncated EGFR.

To characterize the transcript encoding for this putative EGFR variant, long-distance RT-PCR was used to amplify *EGFR* cDNAs in EPP and EPP-MI cells. We could detect an amplicon of the expected size for full-length *EGFR* (~4.2 Kb) in both lines, whereas no amplicon using the canonical ATG initiation codon of the *EGFR* transcript and coding for an ~80 kDa protein (expected size ~ 2.4 Kb) was found in the EPP-MI line (Fig. 3B).

We therefore hypothesized that the EGFR variant could be a fusion protein retaining the C-terminus of EGFR downstream to an N-terminus of an unknown protein. To resolve the identity of the gene fusion, transcriptome analysis on EPP and EPP-MI lines was performed, which identified an open reading frame resulting from an *SEC61G-EGFR* gene fusion joining the 5′-UTR of *SEC61G* (NM_014302) and exon 14 of *EGFR* (NM_005228; Fig. 3C). The two genes are located on chromosome 7 and reside adjacent to one another in opposite orientation. PCR amplification and Sanger sequencing identified two distinct fusion mRNAs, arising from in-frame splicing of the 5′-UTR of *SEC61G* upstream of either exon 14 or exon 15 of *EGFR* (Fig. 3B and D). Skipping of exon 16 was present in both mature mRNAs, with maintenance of the reading frame to the canonic stop codon within EGFR exon 28. The two mRNAs, which likely originate from alternative splicing of *SEC61G-EGFR* transcript, were predicted to encode for two novel fusion products, EGFRΔN566 (GenBank MF434546) and EGFRΔN599 (GenBank MF434547), which retain the transmembrane and the kinase domain of EGFR, but lack the extracellular ligand-binding region almost completely (Fig. 3E).

By using a nested RT-PCR assay, we confirmed the presence of the *SEC61G–EGFR* gene fusion found in EPP-MI line also in the corresponding MD line. Specifically, the chimeric mRNAs were present at high levels in EPP-MI cells and at very low levels in EPP, where they were detected only after the second round of

amplification (Supplementary Fig. S2B and S2C). In the EPP line, *SEC61G–EGFR* mRNAs had been retained through serial passages, with their level being positively modulated by growth factor deprivation (Supplementary Fig. S2C).

We finally addressed the molecular features underlying the constitutive activation of EGFRΔN566/EGFRΔN599 or full-length EGFR observed in MI cells. Enhanced signal mediated by EGFR can occur through overexpression of the receptor or cognate ligands (EGF and TGFA), heterodimerization with other EGFR family members (HER2, HER3, or HER4) or be due to mutations promoting constitutive catalytic activity (17). Sequencing of the entire region coding for the catalytic domain of *EGFR* ruled out the presence of point mutations or small indels predicted to drive hyperactive behavior of the receptor in both MI lines. Quantitative PCR analysis revealed that *EGF*, *HER2 (ERBB2)*, and *HER4* (*ERBB4*) were expressed at similar and very low levels in all paired MD and MI lines, whereas *HER3* (*ERBB3*) and *TGFA* were even diminished in MI lines (Supplementary Fig. S2D). Together, these data suggest that constitutive activation of full-length (in EPV-FL-MI cells) or truncated EGFR (in EPP-MI cells) is likely due to receptor overexpression, accompanied by loss of autoinhibitory regulation in EGFRΔN566/EGFRΔN599.

SEC61G–EGFR fusion is present in pediatric ependymomas

To assay for the presence of *SEC61G–EGFR* fusion in pediatric ependymomas, we screened 16 tumor specimens from 15 patients by nested RT-PCR assay, including the tumor (EPM1) from which the lines harboring the rearrangement had been derived. The first round of PCR with specific primers for *SEC61G–EGFR* showed chimeric mRNAs in one recurrent infratentorial ependymoma WHO III (EPM6), but not in EPM1 (Fig. 4A). We interpret this finding as likely due to high intratumor heterogeneity for *SEC61G–EGFR* fusion. The second round of PCR and Sanger sequencing confirmed the presence of the fusion gene only in the positive sample, and apparently excluded that *SEC61G–EGFR* fusions could be expressed at very low levels in the other samples. Overall, these data support the view that *SEC61G–EGFR* chimeric products are likely to have a heterogeneous intratumor pattern, similar to other EGFR alterations in neural tumors (29–31). The small number of samples analyzed for the presence of the *SEC61G–EGFR* fusion does not allow definitive conclusions regarding the frequency of this genetic event in ependymomas.

We finally analyzed the expression of EGFR in EPM1 and EPM6 by immunofluorescence. EPM6 displayed strong positivity for EGFR in the majority of tumor cells, whereas EPM1, which had scored negative in the RT-PCR assay, exhibited positive staining only in discrete clusters of cells (Fig. 4B and C).

EPP-MI line stably maintains the expression of EGFRΔN566/EGFRΔN599

To further characterize EGFRΔN566/EGFRΔN599, we investigated its expression pattern *in vitro* and *in vivo* by immunofluorescence using EGFR-C and EGFR-N antibodies (Fig. 5A–C). Cytological comparison of EPP and EPP-MI lines showed that the first displayed an overlapping pattern of EGFR expression with both antibodies; by contrast, the EPP-MI line exhibited a diffuse staining with EGFR-C antibody, whereas only few cells reacted with both EGFR-N and EGFR-C antibodies (Fig. 5A and C). These data indicate that the EPP-MI line is mostly made up of cells expressing EGFRΔN566/EGFRΔN599, with rare cells either expressing full-length EGFR or coexpressing full-length and truncated EGFR. The pattern of staining *in vitro* was similar to that observed in intracranial EPP and EPP-MI tumors: an evenly distributed labeling with both antibodies was evident in EPP tumors (Fig. 5B and C), whereas in EPP-MI tumors a high and diffuse staining was observed with EGFR-C antibody, which colocalized with anti–EGFR-N antibody in some cells. A small percentage of cells (~10%) reacted only with anti–EGFR-N in EPP-MI xenografts.

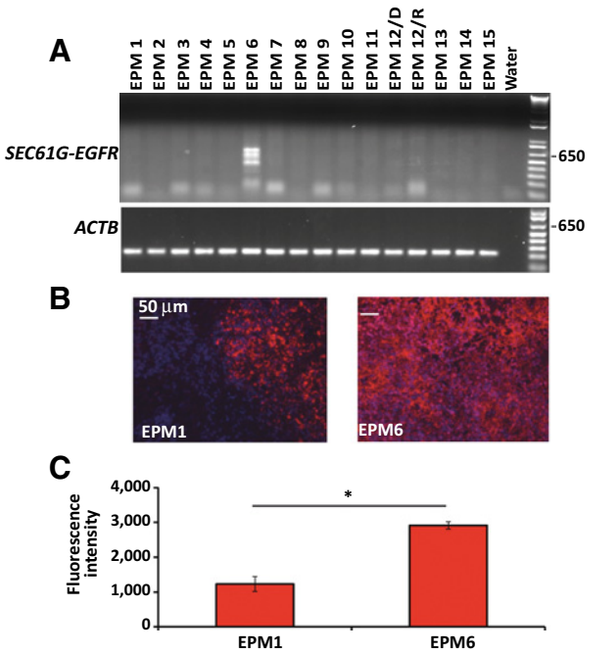

Figure 4.

SEC61G–EGFR fusion transcript is expressed in pediatric ependymoma. **A,** *SEC61G–EGFR* exon 19–specific PCR from cDNAs derived from ependymoma samples. Amplification of the housekeeping gene *ACTB* is shown. Water was used as a negative control for the PCR. **B,** Representative microphotographs of EGFR immunofluorescence in *SEC61G–EGFR*-negative (EPM1) and -positive (EPM6) samples using an antibody that recognizes the C-terminus of EGFR. Scale bar, 50 μm. **C,** Quantitation of staining of the above images was performed using Cellsens Dimension software from Olympus. The Student *t* test was used for statistical significance. *, $P < 0.001$.

To address whether EGFRΔN566/EGFRΔN599 is a stable molecular feature of EPP-MI cells, we reestablished lines from intracranial and subcutaneous tumors driven by EPP-MI and EPP cells and determined EGFR expression by Western blot analysis. Cultures derived from both orthotopic and heterotopic xenografts exhibited EGFR expression similar to that of the corresponding patient-derived cell cultures (Supplementary Fig. S3A), i.e., full-length EGFR in the lines established from EPP-tumors and truncated EGFR in those established from EPP-MI tumors. Of note, the expression of EGFRΔN566/EGFRΔN599 was not affected by culturing EPP-MI intracranial or subcutaneous tumor cells in either MFM or SCM, neither did it differ in lines established from the two *in vivo* models. In addition, EPP-MI cells exhibited a higher tumor growth rate than EPP also after heterotopic implantation, indicating that increased tumorigenicity is a niche-independent feature of this line (Supplementary Fig. S3B). Together, these data support the view that the EPP-MI line, which stably expresses the gene fusion product, might represent a subpopulation of the EPP

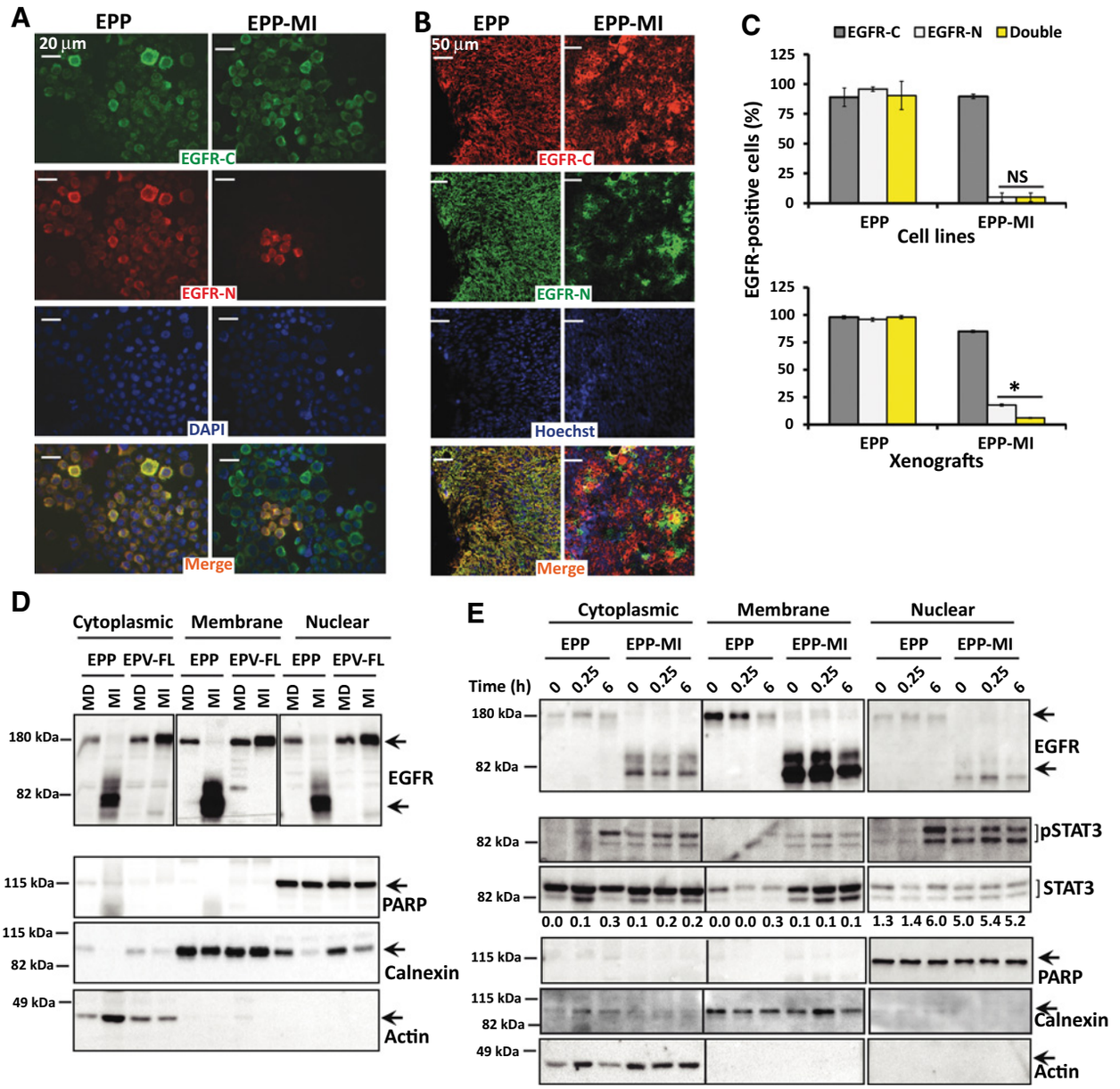

Figure 5.

Characterization of EGFRΔN566/EGFRΔN599 in EPP-MI cells. **A,** EGFR labeling in EPP and EPP-MI cells *in vitro* using antibodies that recognize epitopes at either the N-terminus (EGFR-N) or C-terminus (EGFR-C) of EGFR. Nuclei were counterstained with DAPI. Scale bar, 20 μm. **B,** EGFR labeling on intracranial tumor sections of mice injected with EPP and EPP-MI cells. Brains were processed when animals developed brain tumor symptoms approximately 75 and 25 days after implantations of equal numbers of EPP and EPP-MI cells. EGFR expression was detected by using the primary antibodies described above. Nuclei were counterstained with Hoechst. Scale bar, 50 μm. **C,** EGFR staining in **A** and **B** was quantitated by counting at least 5 × 100 cells from representative fields and was expressed as the average percent positive. The Student *t* test was used for statistical significance. NS, not significant; *, $P < 0.001$. **D** and **E,** Subcellular localization of EGFR and EGFRΔN566/EGFRΔN599 in ependymoma lines. **D,** MD and MI lines were grown in SCM and MFM, respectively. Samples were subjected to subcellular fractionation to obtain cytoplasmic, membrane, and nuclear extracts and analyzed by immunoblot using EGFR-C antibody. Short and prolonged exposures are shown for membrane or cytoplasmic and nuclear extracts, respectively. **E,** EPP and EPP-MI cells were mitogen-starved for 48 hours and then treated with 25 ng/mL EGF for the indicated times. Samples were subject to subcellular fractionation as in **D**. Blots were probed with the indicated antibodies. Efficacy of subcellular fractionation in **D** and **E** is indicated by cytoplasmic marker protein actin, membrane marker protein calnexin, and nuclear marker protein PARP. Densitometry analysis of the bands was performed using Image Lab software (Bio-Rad Laboratories Inc.). The numbers below the panels represent the expression levels of phosphorylated STAT3 (pSTAT3) normalized to STAT3. One representative experiment out of two is shown.

line. However, a functional state of SCs cannot be excluded, mostly in the EPV-FL-MI line.

EGFRΔN566/EGFRΔN599 is associated with EGF-independent activation of nuclear STAT3

Subcellular localization of EGFRΔN566/EGFRΔN599 in EPP-MI cells paralleled that of full-length EGFR in the other lines, being the majority of the proteins bound to membranes, and much lower amounts recovered in the cytoplasmic and nuclear fractions (Fig. 5D). Because STAT3 is a mediator of EGFR signaling through physical interaction and functional cooperation with EGFR and EGFR mutants (32), we analyzed the subcellular localization and activation status of STAT3 without and with EGF in EPP and EPP-MI lines. In the absence of EGF, EGFR and EGFRΔN566/EGFRΔN599 were mainly detected in the membrane extracts (Fig. 5E). EGF treatment resulted in a time-dependent decrease in the membrane-associated receptors in both lines, with no substantial difference in the cytoplasmic and nuclear EGFR and EGFRΔN566/EGFRΔN599. Prolonged exposure to EGF promoted STAT3 phosphorylation in cytoplasmic, membrane, and nuclear protein extracts in EPP cells, without increasing STAT3 expression in any of the fractions. In contrast, STAT3 was constitutively active in all subcellular compartments in EPP-MI cells, with highest levels in the nucleus, nor was it further induced by EGF treatment. Amounts of cytoplasmic and nuclear STAT3 were similar in EPP and EPP-MI lines, whereas the membrane fraction of STAT3 was much higher in EPP-MI.

Constitutively active signaling through EGFR and EGFRΔN566/EGFRΔN599 is efficiently suppressed by EGFR TKIs in MI ependimoma lines

We compared EGFR-mediated signaling in MD and MI cell lines in the absence (MFM) and presence of EGF. In MFM, EGFR and downstream signaling molecules (STAT3, AKT, and ERK1/2) displayed low levels of activation in MD cells, whereas constitutive activation of either EGFRΔN566/EGFRΔN599 or EGFR in EPP-MI or EPV-FL-MI lines, respectively, correlated with overactivation of STAT3 and AKT, but had no significant effect on ERK1/2 (Fig. 6; Supplementary Fig. S4A and S4B). Addition of EGF triggered the canonical signaling cascade through activation of EGFR, AKT, and ERK1/2 in MD lines. By contrast, no induction above the baseline levels was evident in EPP-MI cells, apart from a little increase in phosphorylated full-length EGFR. In EPV-FL-MI, constitutive phosphorylation of the receptor was further increased by EGF, with a parallel activation of AKT and ERK1/2.

The EGFR TKIs AEE788 (Fig. 6) and gefitinib (Supplementary Fig. S4B) prevented ligand-triggered phosphorylation of EGFR, AKT, and ERK1/2 dose dependently in MD lines, in agreement with our published data in EPP cells (14). Both agents also fully suppressed the constitutive activation of EGFR and EGFRΔN566/EGFRΔN599 in MI lines, reducing in parallel the levels of phosphorylated AKT and ERK1/2.

As for STAT3, it was unresponsive to EGF stimulation in all lines, and its constitutive activation in MI lines was partially inhibited by both EGFR-targeted agents only in EPP-MI cells. Interestingly, phosphorylated STAT3 was present in MD cells grown in SCM and reduced by mitogen starvation. These data, together with the delayed, yet remarkable, activation of nuclear STAT3 in EPP following prolonged EGF exposure (Fig. 5E), and the only partial response to EGFR inhibitors in MI lines in spite of high constitutive STAT3 activation, suggest that other pathways converge on STAT3 in ependymoma cells in addition to EGFR.

No substantial difference in the abundance of total STAT3, AKT, and ERK1/2 was observed among lines and conditions; by contrast, the amounts of total EGFR were markedly different in lines grown in MFM compared with SCM. Specifically, MFM determined upregulation of EGFR expression in MD lines, without altering its phosphorylation status. On the other hand, SCM decreased EGFR expression and activation in EPV-FL-MI, these data reinforcing the view of a predominant ligand-independent activation of EGFR signaling in this line. Levels of total and phosphorylated EGFRΔN566/EGFRΔN599 were substantially unchanged in the two culturing conditions.

To further explore the effects of EGFR TKIs on ligand-independent signaling mediated by EGFRΔN566/EGFRΔN599, we compared the activation profile in EPP and EPP-MI lines in MFM (Supplementary Fig. S4C). In EPP cells, only AKT basal activation was reduced to some extent by both TKIs; in contrast, a significant loss of signals downstream to EGFR occurred in EPP-MI cells, where the activation of AKT and ERK1/2 decreased in parallel with that of EGFRΔN566/EGFRΔN599. Activated STAT3 was less responsive to pharmacological inhibition.

Ependymoma lines with ligand-independent EGFR signaling are specifically sensitive to the antiproliferative effects of EGFR TKIs *in vitro* and *in vivo*

Constitutive activation of EGFR confers sensitivity to EGFR TKIs in cell lines from different tumors, including glioblastoma (33–35). No data are available in ependymoma lines. To address whether treatment with EGFR TKIs differentially affects the proliferation of cells with ligand-dependent versus ligand-independent EGFR signaling, we exposed MD and MI lines to serial concentrations of gefitinib or AEE788. Both agents exerted a dose-dependent reduction in the number of viable cells with a concomitant increase in the number of nonviable cells (Fig. 7A and B; Supplementary Fig. S5A and S5B). Graph plots and IC_{50} values indicated that MI lines were up to 3-fold more sensitive to the antiproliferative effects of both agents than their counterparts, being the EPP-MI line, which harbors EGFRΔN566/EGFRΔN599, 2-fold more responsive than EPV-FL-MI (Supplementary Table S2).

To further assess whether EGFRΔN566/EGFRΔN599 could represent a druggable target by EGFR TKIs, we compared the cellular events elicited by AEE788 in EPP and EPP-MI cells. Long-term exposure to 1 μmol/L AEE788 induced apoptosis in EPP cells, as detected by the cleavage of PARP (Fig. 7C), confirming our previous findings (14). In EPP-MI cells, AEE788 was able to promote earlier onset of apoptosis, because PARP cleavage occurred after a 3-day treatment and at a lower dose (Fig. 7C). Although AEE788 irreversibly blocked the catalytic activity of EGFR and EGFRΔN566/EGFRΔN599, it determined upregulation of EGFR in EPP cells, while decreasing the amounts of EGFRΔN566/EGFRΔN599 in EPP-MI cells.

Finally, we addressed whether the differential effects of EGFR blockade observed in EPP and EPP-MI cultures translate to *in vivo* survival difference by targeting EGFR in intracranial tumor growth. In agreement with our previously published data (14), orally administered AEE788 did not exert any antitumor activity on orthotopic EPP-driven tumors (log-rank, $P = 0.7$), whereas it determined a statistically significant prolongation of survival of mice bearing EPP-MI xenografts (log-rank, $P = 0.0002$; Fig. 7D).

AEE788 reduced the proliferating fraction in EPP-MI xenografts, as evidenced by a significant decrease in the percentage of Ki-67 positive tumor cells in histological preparations from drug-treated animals (Fig. 7E and F). Staining with EGFR-C and EGFR-N antibodies demonstrated that AEE788 mostly targeted cells expressing mutant EGFR, because the percentage of EGFR-C

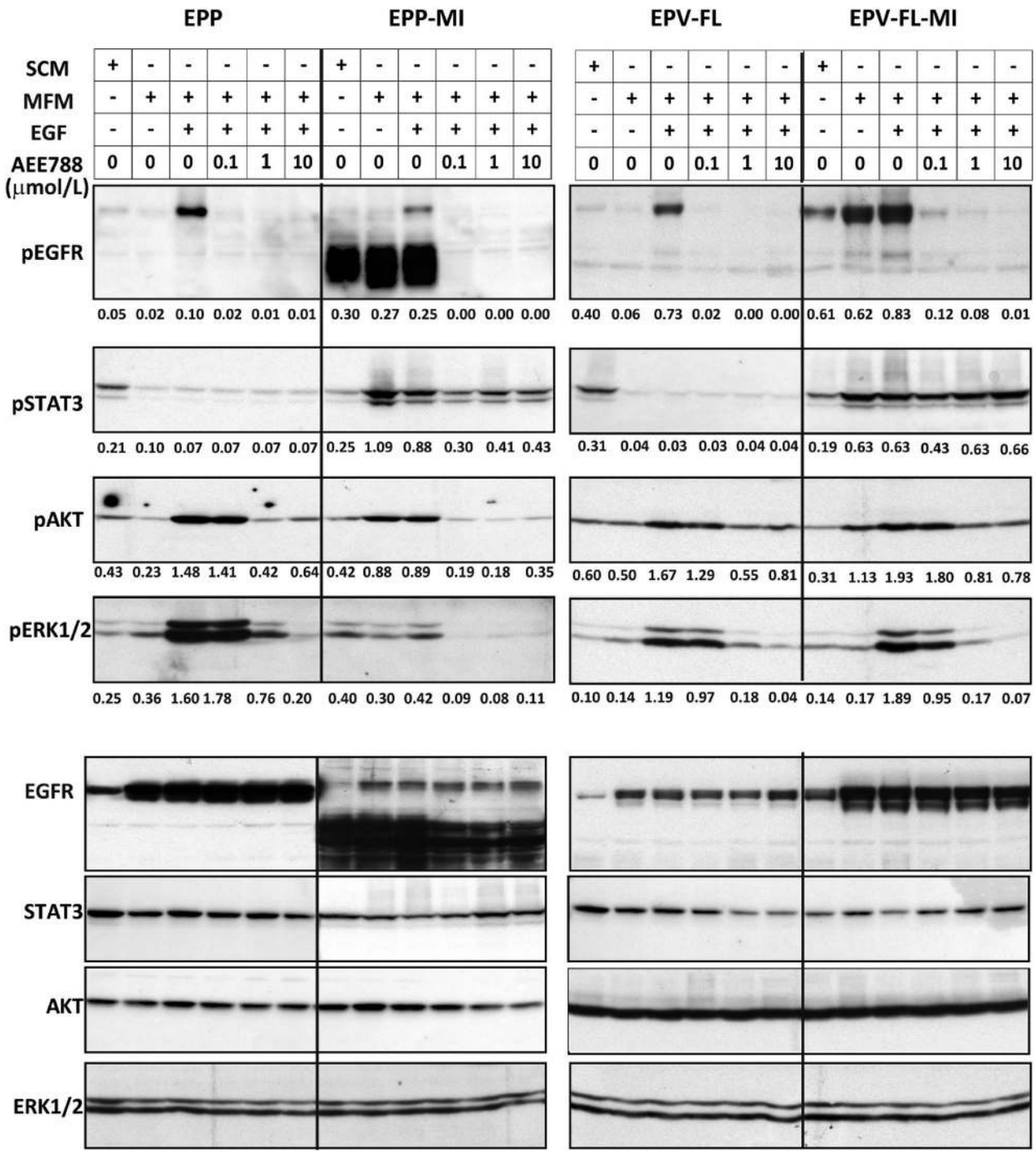

Figure 6.

EGFR and EGFRΔN566/EGFRΔN599 are constitutively active in MI ependymoma lines and are blocked by the EGFR TKI AEE788. Cells were grown in SCM or MFM for 48 hours. Mitogen-starved cells were then treated with increasing concentrations of AEE788 for 2 hours prior to a 10-minute stimulation with 25 ng/mL EGF. Cell lysates were subjected to immunoblot analysis with antibodies to phosphorylated (p) and total EGFR (EGFR-C), STAT3, AKT, and ERK1/2. Densitometry analysis of the bands was performed using ImageJ. The numbers below the panels represent the relative expression of each phosphorylated protein to the corresponding total protein. One representative experiment out of at least two is shown.

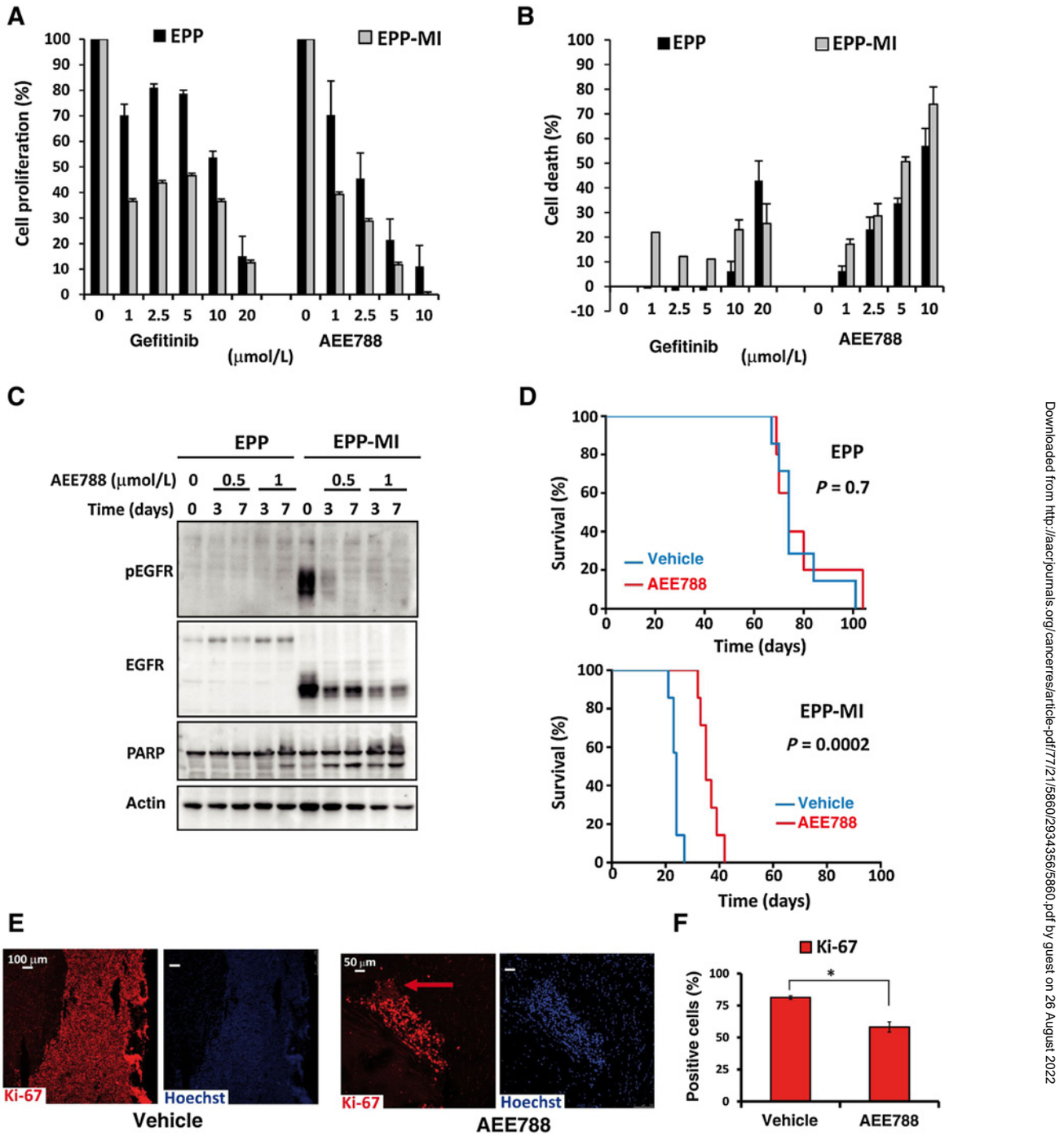

Figure 7.

EGFRΔN566/EGFRΔN599 expression confers sensitivity to *in vitro* and *in vivo* targeting with EGFR TKIs. **A,** Dose-dependent antiproliferative effects of the indicated EGFR TKIs in EPP and EPP-MI lines, harboring either full-length EGFR or EGFRΔN566/EGFRΔN599, respectively. Cells were treated with the indicated drug concentrations for 72 hours (mean ± SD, $n = 6$). **B,** Cell death of the sensitive assays shown in **A**. **C,** Time course of the effects exerted by AEE788 on the activation of PARP and EGFR or EGFRΔN566/EGFRΔN599 in EPP and EPP-MI lines, respectively. Cells were exposed to the indicated concentrations of AEE788 for 3 or 7 days. Cell lysates were subjected to immunoblot analysis with the indicated antibodies. **D**, Survival analysis of mice bearing orthotopic EPP or EPP-MI xenografts. Animals were treated with orally administered vehicle or AEE788 (50 mg/kg daily for 5 days for 4 weeks; $n = 8$ mice/group). On the appearance of brain tumor symptoms, animals were sacrificed. Survival was examined using the Kaplan–Meier method. **E,** Ki-67 staining of intracranial EPP-MI tumor sections from mice treated with vehicle or AEE788. Scale bar, 100 μm or 50 μm, respectively. Red arrow, Ki-67–negative tumor cells. **F,** Quantitation of Ki-67 staining shown in **E**. At least 5 × 100 cells were counted in five nonconsecutive sections of each histological preparation. Ki-67 staining was expressed as the percentage of Ki-67–positive cells with respect to Hoechst stained cells of the same sections. Student *t* test was used for statistical significance. *, $P < 0.001$; significantly different from the sections of vehicle-treated animals.

positive cells was significantly reduced, whereas the percentage of double-positive cells was unchanged and that of EGFR-N positive cells increased (Supplementary Fig. S6A and S6B). These cells likely express N-terminus soluble isoform(s) of EGFR, that we found only *in vivo*, probably as the product of alternative splicing (36–38). No statistically significant change in the percentage of the different EGFR isoforms was evident in EPP xenografts after AEE788 administration.

Overall, *in vitro* and *in vivo* data support the idea that constitutive activation of EGFR signal in ependymoma, including that one driven by EGFR mutants, might be therapeutically targeted by EGFR TKIs.

Discussion

In this study, we provide evidence that autonomous proliferative and prosurvival behavior of ependymoma SCs is mediated by EGFR through mechanisms altering both the expression and the control of the catalytic activity of the receptor, although other pathways might be involved. Constitutively active EGFR and EGFRΔN566/EGFRΔN599 are associated with overactivation of AKT and STAT3, sensitization to EGFR TKIs and increased tumorigenicity. The growth advantage of ependymoma SCs expressing activated EGFR or EGFRΔN566/EGFRΔN599 is observed only *in vivo*, in agreement with previous findings in MI glioblastoma SCs with high-level *EGFR* amplification/EGFRvIII expression (23). These results suggest that alterations of EGFR signaling play an important role in tumor progression, possibly by influencing interactions of tumor cells with their microenvironment.

From both the structural and functional standpoints, the newfound *SEC61G–EGFR* gene fusion products EGFRΔN566/EGFRΔN599 resemble the well-characterized EGFRvIII, which lacks part of the extracellular domain, is constitutively phosphorylated and signals through overactivation of AKT and nuclear STAT3 (32, 33). Alike EGFRvIII, EGFRΔN566/EGFRΔN599 potently accelerate tumor growth, but they also sensitize ependymoma cells to the antiproliferative effects of EGFR TKIs both *in vitro* and *in vivo* (33, 35). Continuous treatment with EGFR TKIs was found to cause a marked decrease in the levels of EGFRΔN566/EGFRΔN599, while inducing upregulation of full-length EGFR. In EGFRvIII-expressing glioblastoma, EGFR TKIs cause loss of EGFRvIII in cell lines and tumor tissues from treated patients, suggesting that depletion of EGFRvIII might be a clinically relevant mechanism of resistance to the pharmacological blockade of EGFR signaling (35). By the same token, it is tempting to speculate that EGFRΔN566/EGFRΔN599 expression might identify a subpopulation of ependymoma cells potentially responsive to inhibition of EGFR signaling. However, our finding that STAT3 is only partially inhibited suggests that EGFR targeting alone could not suffice to inhibit tumor growth.

The relative resistance of STAT3 to EGFR TKIs is in agreement with findings in other tumor cell lines that express mutant EGFR, where gefitinib is able to suppress EGFR, ERK1/2, and AKT phosphorylation, but less so STAT3 phosphorylation (39). A variety of stimuli converge on STAT3, including growth factors and cytokines, and research in the STAT3 pathway has far largely broadened the mechanisms by which this transducer is activated (40). Human glioma tissues and SCs that express EGFRvIII also express IL6, the prototypical activator of STAT3 (41). Constitutive IL6/STAT3 activation drives growth of high-risk ependymomas (42). In different tumors, aberrant EGFR signaling promotes activation of NF-κB, which is functionally linked to STAT3 (43, 44). In addition to EGFR, other pathways likely drive STAT3 activation in MI ependymoma lines, suggesting that the therapeutic efficacy of EGFR TKIs in tumors with EGFR mutants and/or activated EGFR could improve with concomitant inhibition of STAT3.

EGFRΔN566/EGFRΔN599 were identified in one ependymoma SC line exhibiting high tumorigenicity, in spite of an overall decrease in the expression of stemness markers, including CD133. Although CD133 is a defining marker for cancer SCs, we have shown that CD133 expression does not segregate with tumorigenicity in ependymoma SCs (14, 26). Here, we demonstrate that the activation/expression of full-length or truncated EGFR correlates with tumor-initiating property of ependymoma SCs, possibly explaining why the EPV-MI line, which does not display EGFR activation, does not exhibit a more malignant phenotype. On the whole, our data are in agreement with findings in glioblastoma SCs, where EGFR expression positively correlates with *in vivo* tumor growth more than CD133 expression (45).

Notably, RT-PCR sequencing of 16 pediatric ependymomas identified *SEC61G–EGFR* fusion in one infratentorial tumor WHO III. Our limited cohort of patients does not allow determining an accurate estimate of the frequency of *SEC61G–EGFR* fusions in childhood ependymomas, and further efforts are required to establish the clinical relevance of this event in this malignancy. So far, only two fusions have been discovered in ependymomas, which involve either the *YAP1* or *RELA* genes, and characterize two distinct tumor subgroups both arising in the supratentorial compartment (8, 46). More recently, the novel *TSPAN4-CD151* fusion gene has been identified in one pediatric infratentorial anaplastic ependymoma through RNA-seq and PCR validation, although the functional importance of the fusion has not been addressed (47). The *SEC61G–EGFR* fusion here characterized involves two genes that are normally positioned on chromosome 7p11, approximately 0.26 megabases away from each other. *SEC61G–EGFR* fusions have been reported in 4 of 164 glioblastoma transcriptomes (2.4%); however, neither chimeric products nor functional data have been provided (48). Interestingly, 29% of the mRNA fusion transcripts found in this study involve 3′ or 5′ untranslated regions, and a high percentage (44%) of the intrachromosomal rearrangements results from recombination of genomic loci distant less than 1 megabase from one another (48).

In the last decade, high-throughput genomic, transcriptional, and epigenetic analyses have highlighted the complex genetic landscape of ependymomas (8–12, 46). However, subclonal molecular mutations might go undetected by DNA and RNA sequencing of bulk tumors, taking into account that tumors usually consist of multiple clonal populations often residing among genetically normal noncancerous cells (30, 49–51). A mosaic pattern of EGFR aberrations at both genomic and transcriptomic levels has been identified through single-cell DNA and RNA sequencing in glioblastoma (52, 53). Cell lines generated from glioblastoma with heterogeneous pattern of expression/amplification of receptor tyrosine kinases exhibit genotype selection under receptor-targeted ligand stimulation (22, 23, 30). Here, we show that clonal expansion of tumor-derived cells through differential selective pressure exerted by culture conditions can successfully be used in ependymomas as a

complementary strategy to uncover intratumor genetic heterogeneity and identify novel alterations contributing to the pathogenetic mechanisms and drug sensitivity of this malignancy.

In conclusion, our work documents that constitutive activation of EGFR and of its downstream signaling pathways mediated by AKT and STAT3 is associated with mitogen independence and a more aggressive behavior of ependymoma SCs. Enhanced levels of EGFR and phosphorylated STAT3 occur in patients with ependymoma, especially in the anaplastic histology group (20, 21, 54). Together, these data suggest that the EGFR/STAT signaling axis might be essential to dictate the transcriptional profile of more malignant ependymoma cells and might be therapeutically targeted. *SEC61G–EGFR* is the first fusion that has been described at both molecular and functional levels in infratentorial ependymomas and represents the first instance of an EGFR fusion that is endogenously expressed by ependymoma SCs. Further studies are necessary to define its prevalence in these neoplasms and assess its overall clinical relevance.

Disclosure of Potential Conflicts of Interest

No potential conflicts of interest were disclosed.

Authors' Contributions

Conception and design: T. Servidei, M. Caldarelli, R. Riccardi
Development of methodology: T. Servidei,
Acquisition of data (provided animals, acquired and managed patients, provided facilities, etc.): T. Servidei, D. Meco, V. Muto, N. Trivieri, M. Caldarelli, A. Lasorella, R. Riccardi
Analysis and interpretation of data (e.g., statistical analysis, biostatistics, computational analysis): T. Servidei, D. Meco, V. Muto, A. Bruselles, A. Ciolfi, M. Lucchini, R. Morosetti, M. Mirabella, M. Martini, A. Lasorella, M. Tartaglia, R. Riccardi
Writing, review, and/or revision of the manuscript: T. Servidei, V. Muto, A. Bruselles, A. Ciolfi, M. Lucchini, R. Morosetti, M. Mirabella, M. Tartaglia, R. Riccardi
Administrative, technical, or material support (i.e., reporting or organizing data, constructing databases): T. Servidei, R. Riccardi
Study supervision: T. Servidei, M. Caldarelli, M. Tartaglia, R. Riccardi

Acknowledgments

We are grateful to Dr. Giuseppe Lamorte for performing cytofluorimetric analyses.

Grant Support

This work was supported by Fondazione per l'Oncologia Pediatrica (to T. Servidei) and by Associazione Italiana per la Ricerca sul Cancro (IG17583 to M. Tartaglia).

The costs of publication of this article were defrayed in part by the payment of page charges. This article must therefore be hereby marked *advertisement* in accordance with 18 U.S.C. Section 1734 solely to indicate this fact.

Received March 17, 2017; revised July 13, 2017; accepted August 30, 2017; published online November 1, 2017.

References

1 Kilday JP, Rahman R, Dyer S, Ridley L, Lowe J, Coyle B, et al. Pediatric ependymoma: biological perspectives. Mol Cancer Res 2009;7:765–86.
2 Korshunov A, Witt H, Hielscher T, Benner A, Remke M, Ryzhova M, et al. Molecular staging of intracranial ependymoma in children and adults. J Clin Oncol 2010;28:3182–90.
3 Gatta G, Botta L, Rossi S, Aareleid T, Bielska-Lasota M, Clavel J, et al. EUROCARE working group. Childhood cancer survival in Europe 1999–2007: results of EUROCARE-5—a population-based study. Lancet Oncol 2014;15:35–47.
4 Grundy RG, Wilne SA, Weston CL, Robinson K, Lashford LS, Ironside J, et al. Primary postoperative chemotherapy without radiotherapy for intracranial ependymoma in children: the UKCCSG/SIOP prospective study. Lancet Oncol 2007;8:696–705.
5 Gajjar A, Pfister SM, Taylor MD, Gilbertson RJ. Molecular insights into pediatric brain tumors have the potential to transform therapy. Clin Cancer Res 2014;20:5630–40.
6 Northcott PA, Pfister SM, Jones DT. Next-generation (epi)genetic drivers of childhood brain tumours and the outlook for targeted therapies. Lancet Oncol 2015;16:e293–302.
7 Louis DN, Ohgaki H, Wiestler OD, Cavenee WK, Burger PC, Jouvet A, et al. The 2007 WHO classification of tumours of the central nervous system. Acta Neuropathol 2007;14:97–109.
8 Pajtler KW, Witt H, Sill M, Jones DT, Hovestadt V, Kratochwil F, et al. Molecular classification of ependymal tumors across all CNS compartments, histopathological grades, and age groups. Cancer Cell 2015;27:728–43.
9 Taylor MD, Poppleton H, Fuller C, Su X, Liu Y, Jensen P, et al. Radial glia cells are candidate stem cells of ependymoma. Cancer Cell 2005;8:323–35.
10 Modena P, Lualdi E, Facchinetti F, Veltman J, Reid JF, Minardi S, et al. Identification of tumor-specific molecular signatures in intracranial ependymoma and association with clinical characteristics. J Clin Oncol 2006;24:5223–33.
11 Witt H, Mack SC, Ryzhova M, Bender S, Sill M, Isserlin R, et al. Delineation of two clinically and molecularly distinct subgroups of posterior fossa ependymoma. Cancer Cell 2011;20:143–57.
12 Mack SC, Witt H, Piro RM, Gu L, Zuyderduyn S, Stütz AM, et al. Epigenomic alterations define lethal CIMP-positive ependymomas of infancy. Nature 2014;7489:445–50.
13 Vescovi AL, Galli R, Reynolds BA. Brain tumour stem cells. Nat Rev Cancer 2006;6:425–36.
14 Servidei T, Meco D, Trivieri N, Patriarca V, Vellone VG, Zannoni GF, et al. Effects of epidermal growth factor receptor blockade on ependymoma stem cells *in vitro* and in orthotopic mouse models. Int J Cancer 2012;131:E791–803.
15 Yarden Y, Sliwkowski MX. Untangling the ErbB signalling network. Nat Rev Mol Cell Biol 2001;2:127–37.
16 Schlessinger J. Ligand-induced, receptor-mediated dimerization and activation of EGF receptor. Cell 2002;110:669–72.
17 Guo G, Gong K, Wohlfeld B, Hatanpaa KJ, Zhao D, Habib AA. Ligand-independent EGFR signaling. Cancer Res 2015;75:3436–41.
18 Nishikawa R, Ji XD, Harmon RC, Lazar CS, Gill GN, Cavenee WK, et al. A mutant epidermal growth factor receptor common in human glioma confers enhanced tumorigenicity. Proc Natl Acad Sci U S A 1994;91:7727–31.
19 Verhaak RG, Hoadley KA, Purdom E, Wang V, Qi Y, Wilkerson MD, et al. Integrated genomic analysis identifies clinically relevant subtypes of glioblastoma characterized by abnormalities in PDGFRA, IDH1, EGFR, and NF1. Cancer Cell 2010;17:98–110.
20 Mendrzyk F, Korshunov A, Benner A, Toedt G, Pfister S, Radlwimmer B, et al. Identification of gains on 1q and epidermal growth factor receptor overexpression as independent prognostic markers in intracranial ependymoma. Clin Cancer Res 2006;12:2070–9.
21 Friedrich C, von Bueren AO, Kolevatova L, Bernreuther C, Grob T, Sepulveda-Falla D, et al. Epidermal growth factor receptor overexpression is common and not correlated to gene copy number in ependymoma. Childs Nerv Syst 2016;32:281–90.
22 Kelly JJ, Stechishin O, Chojnacki A, Lun X, Sun B, Senger DL, et al. Proliferation of human glioblastoma stem cells occurs independently of exogenous mitogens. Stem Cells 2009;27:1722–33.
23 Schulte A, Günther HS, Martens T, Zapf S, Riethdorf S, Wülfing C, et al. Glioblastoma stem-like cell lines with either maintenance or loss of high-level EGFR amplification, generated via modulation of ligand concentration. Clin Cancer Res 2012;18:1901–13.
24 Pandita A, Aldape KD, Zadeh G, Guha A, James CD. Contrasting *in vivo* and *in vitro* fates of glioblastoma cell subpopulations with amplified EGFR. Genes Chromosomes Cancer 2004;39:29–36.

25 Traxler P, Allegrini PR, Brandt R, Brueggen J, Cozens R, Fabbro D, et al. AEE788: a dual family epidermal growth factor receptor/ErbB2 and vascular endothelial growth factor receptor tyrosine kinase inhibitor with antitumor and antiangiogenic activity. Cancer Res 2004;64:4931–41.

26 Meco D, Servidei T, Lamorte G, Binda E, Arena V, Riccardi R. Ependymoma stem cells are highly sensitive to temozolomide *in vitro* and in orthotopic models. Neuro-oncology 2014;16:1067–77.

27 D'Antonio M, D'Onorio De Meo P, Pallocca M, Picardi E, D'Erchia AM, Calogero RA, et al. RAP: RNA-Seq Analysis Pipeline a new cloud-based NGS web application. BMC Genomics 2015;16:S3.

28 Iyer MK, Chinnaiyan AM, Maher CA. ChimeraScan: a tool for identifying chimeric transcription in sequencing data. Bioinformatics 2011;27: 2903–04.

29 Nishikawa R, Sugiyama T, Narita Y, Furnari F, Cavenee WK, Matsutani M. Immunohistochemical analysis of the mutant epidermal growth factor, deltaEGFR, in glioblastoma. Brain Tumor Pathol 2004;21:53–6.

30 Szerlip NJ, Pedraza A, Chakravarty D, Azim M, McGuire J, Fang Y, et al. et al. Intratumoral heterogeneity of receptor tyrosine kinases EGFR and PDGFRA amplification in glioblastoma defines subpopulations with distinct growth factor response. Proc Natl Acad Sci U S A 2012;109:3041–6.

31 Furnari FB, Cloughesy TF, Cavenee WK, Mischel PS. Heterogeneity of epidermal growth factor receptor signalling networks in glioblastoma. Nat Rev Cancer 2015;15:302–10.

32 Fan QW, Cheng CK, Gustafson WC, Charron E, Zipper P, Wong RA, et al. EGFR phosphorylates tumor-derived EGFRvIII driving STAT3/5 and progression in glioblastoma. Cancer Cell 2013;14:438–49.

33 Mellinghoff IK, Wang MY, Vivanco I, Haas-Kogan DA, Zhu S, Dia EQ, et al. Molecular determinants of the response of glioblastomas to EGFR kinase inhibitors. N Engl J Med 2005;353:2012–24.

34 Frattini V, Trifonov V, Chan JM, Castano A, Lia M, Abate F, et al. The integrated landscape of driver genomic alterations in glioblastoma. Nat Genet 2013;45:1141–9.

35 Nathanson DA, Gini B, Mottahedeh J, Visnyei K, Koga T, Gomez G, et al. Targeted therapy resistance mediated by dynamic regulation of extrachromosomal mutant EGFR DNA. Science 2014;343:72–6.

36 Reiter L, Threadgill DW, Eley GD, Strunk KE, Danielsen AJ, Sinclair CS, et al. Comparative genomic sequence analysis and isolation of human and mouse alternative EGFR transcripts encoding truncated receptor isoforms. Genomics 2001;71:1–20.

37 Perez-res M, Valle BL, Maihle NJ, Negron-Vega L, Nieves-Alicea R, Cora EM. Shedding of epidermal growth factor receptor is a regulated process that occurs with overexpression in malignant cells. Exp Cell Res 2008; 314:2907–18.

38 Guillaudeau A, Durand K, Bessette B, Chaunavel A, Pommepuy I, Projetti F, et al. EGFR soluble isoforms and their transcripts are expressed in meningiomas. PLoS One 2012;7:e37204.

39 Chaib I, Karachaliou N, Pilotto S, Codony Servat J, Cai X, Li X, et al. Co-activation of STAT3 and YES-Associated Protein 1 (YAP1) pathway in EGFR-mutant NSCLC. J Natl Cancer Inst 2017;109:djx014.

40 Yu H, Pardoll D, Jove R. STATs in cancer inflammation and immunity: a leading role for STAT3. Nat Rev Cancer 2009;9:798–809.

41 Inda MM, Bonavia R, Mukasa A, Narita Y, Sah DW, Vandenberg S, et al. Tumor heterogeneity is an active process maintained by a mutant EGFR-induced cytokine circuit in glioblastoma. Genes Dev 2010;24:1731–45.

42 Griesinger AM, Josephson RJ, Donson AM, Mulcahy Levy JM, Amani V, Birks DK, et al. Interleukin-6/STAT3 pathway signaling drives an inflammatory phenotype in Group A Ependymoma. Cancer Immunol Res 2015;3:1165–74.

43 Sethi G, Ahn KS, Chaturvedi MM, Aggarwal BB. Epidermal growth factor (EGF) activates nuclear factor-kappaB through IkappaBalpha kinase-independent but EGF receptor-kinase dependent tyrosine 42 phosphorylation of IkappaBalpha. Oncogene 2007;26:7324–32.

44 Grivennikov SI, Greten FR, Karin M. Immunity, inflammation, and cancer. Cell 2010;140:883–99.

45 Mazzoleni S, Politi LS, Pala M, Cominelli M, Franzin A, Sergi L, et al. Epidermal growth factor receptor expression identifies functionally and molecularly distinct tumor-initiating cells in human glioblastoma multiforme and is required for gliomagenesis. Cancer Res 2010;70:7500–13.

46 Parker M, Mohankumar KM, Punchihewa C, Weinlich R, Dalton JD, Li Y6, et al. C11orf95-RELA fusions drive oncogenic NF-κB signalling in ependymoma. Nature 2014;506:451–5.

47 Olsen TK, Panagopoulos I, Gorunova L, Micci F, Andersen K, Kilen Andersen H, et al. Novel fusion genes and chimeric transcripts in ependymal tumors. Genes Chromosomes Cancer 2016;55:944–53.

48 Brennan CW, Verhaak RG, McKenna A, Campos B, Noushmehr H, Salama SR, et al. The somatic genomic landscape of glioblastoma. Cell 2013;155: 462–77.

49 Marusyk A, Almendro V, Polyak K. Intra-tumour heterogeneity: a looking glass for cancer? Nat Rev Cancer 2012;12:323–34.

50 Watson IR, Takahashi K, Futreal PA, Chin L. Emerging patterns of somatic mutations in cancer. Nat Rev Genet 2013;14:703–18.

51 Welch DR. Tumor heterogeneity–a contemporary concept founded on historical insights and predictions. Cancer Res 2016;76:4–6.

52 Francis JM, Zhang CZ, Maire CL, Jung J, Manzo VE, Adalsteinsson VA, et al. EGFR variant heterogeneity in glioblastoma resolved through single-nucleus sequencing. Cancer Discov 2014;4:956–71.

53 Patel AP, Tirosh I, Trombetta JJ, Shalek AK, Gillespie SM, Wakimoto H, et al. Single-cell RNA-seq highlights intratumoral heterogeneity in primary glioblastoma. Science 2014;344:1396–401.

54 Phi JH, Choi SA, Kim SK, Wang KC, Lee JY, Kim DG. Overcoming chemoresistance of pediatric ependymoma by inhibition of STAT3 signaling. Transl Oncol 2015;8:376–86.